Available online at ScienceDirect

Nuclear Engineering and Technology

journal homepage: www.elsevier.com/locate/net

Original Article

Visualization of Crust in Metallic Piping Through Real-Time Neutron Radiography Obtained with Low Intensity Thermal Neutron Flux

Leandro C. Luiz [a,b,*,1], *Francisco J.O. Ferreira* [c,1], *and Verginia R. Crispim* [a,1]

[a] *Nuclear Engineering Program, Federal University of Rio de Janeiro, Horácio Macedo Avenue, 2030, Bloco G, 206, Cidade Universitária, 21941-914, Rio de Janeiro, RJ, Brazil*

[b] *Department of Physics, Federal University of Juiz de Fora, Institute of Exact Science, Spectroscopy Materials Laboratory, José Lourenço Kelmer Street, CEP 36036-900, Juiz de Fora, MG, Brazil*

[c] *National Nuclear Energy Commission, CNEN/IEN, Division Reactors, Hélio de Almeida Street, 75, Ilha do Fundão, 21941-614 Rio de Janeiro, RJ, Brazil*

ARTICLE INFO

Article history:
Received 20 September 2016
Received in revised form
13 December 2016
Accepted 14 December 2016
Available online 30 January 2017

Keywords:
Nondestructive Assays
Real-Time Neutron Radiography
Two-Phase Flow

ABSTRACT

The presence of crust on the inner walls of metallic ducts impairs transportation because crust completely or partially hinders the passage of fluid to the processing unit and causes damage to equipment connected to the production line. Its localization is crucial. With the development of the electronic imaging system installed at the Argonauta/Nuclear Engineering Institute (IEN)/National Nuclear Energy Commission (CNEN) reactor, it became possible to visualize crust in the interior of metallic piping of small diameter using real-time neutron radiography images obtained with a low neutron flux. The obtained images showed the resistance offered by crust on the passage of water inside the pipe. No discrepancy of the flow profile at the bottom of the pipe, before the crust region, was registered. However, after the passage of liquid through the pipe, images of the disturbances of the flow were clear and discrepancies in the flow profile were steep. This shows that this technique added the assembled apparatus was efficient for the visualization of the crust and of the two-phase flows.

1. Introduction

In the past several years, study of two-phase flow regimes has been of great interest in the field of engineering and in the engineering industry. The importance of the forecasting of two-phase flows in the industry process is a significant but extremely complicated task. Different two-phase flow patterns are described in the literature [1,2] with regard to the function of the pipe position, whether vertical or horizontal. The best known setups of two-phase systems (liquid–gas) for vertical piping are bubbly flow, slug flow, churn flow, and annular flow. The presence of crusts in the inner walls of a

* Corresponding author.
E-mail address: mrleandroluiz@hotmail.com (L.C. Luiz).

[1] All authors contributed equally.

http://dx.doi.org/10.1016/j.net.2016.12.018

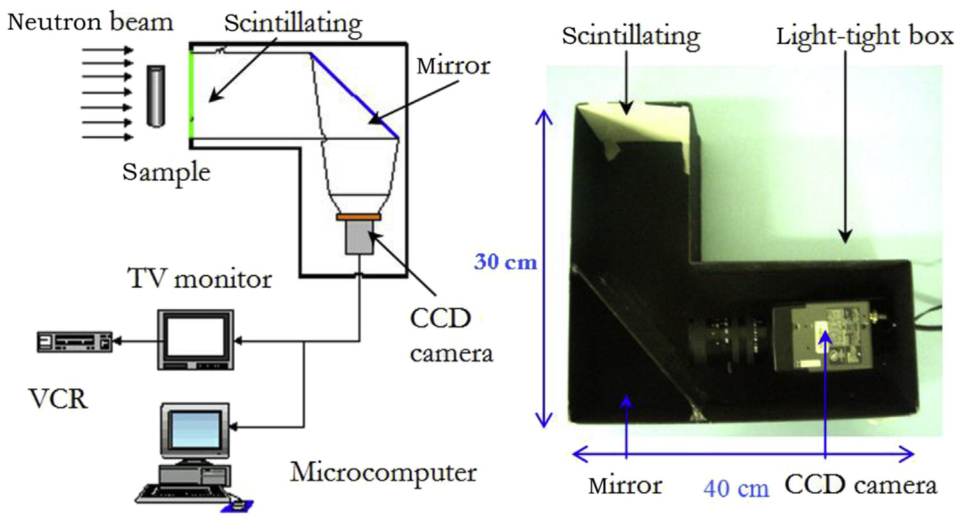

Fig. 1 – Schematic diagram of the real-time neutron radiography EIS installed in the Argonauta reactor (left). Photo of the watertight box that contains the EIS components. CCD, charge coupled device; EIS, electronic imaging system; VCR, videocassette recorder (right).

duct impairs the transportation process of a fluid because such crusts completely or partially hinder the passage of fluid, causing damage to equipment connected to the production line. Obviously, the exact localization of these crusts by nondestructive method can save time, money, and workload for companies acting in the engineering and industry sectors in terms of repairs necessary due to the presence of crust. Neutron radiography (NR) is a nondestructive test method that has been applied in special cases of inspection, in which it is difficult to use other methods such as obtaining radiographs using X-rays or gamma rays [3]. To inspect dynamic events it becomes necessary to have a system that is capable of recording images in real time [4,5]. The objective of this study was to visualize disturbances caused during water flow in aluminum ducts with small internal diameter damaged by crust using the real-time neutron radiography technique. In this manner, we used the electronic imaging system (EIS) developed and installed at the J-9 irradiation channel of the Argonauta/Nuclear Engineering Institute (IEN)/National Nuclear Energy Commission (CNEN) research reactor [6] and spheres that simulated different types of crusts in terms of the interaction of thermal neutrons with the materials that compose them.

2. Materials and methods

2.1. *Real-time neutron radiography setup*

An NR system consists of a thermal neutron beam, a collimator, a sample to be inspected, and a device capable of registering the information on the transmission of neutron beams through the sample. Visualization of flows in the interior of metallic piping has been made possible by the development and installation of the real-time EIS in the Argonauta research reactor. The main system is the thermal neutron beam of the Argonauta/IEN/CNEN reactor, which was used as a neutron source, operating at a nominal power of 340 W and providing a thermal neutron flux of 4.46×10^5 n/cm^2/s at the edge of the J-9 irradiation channel. The Length/Diameter (L/D) ratio of the neutron beam was 70 and the neutron/gamma (n/γ) ratio was 3×10^6 n/cm^2. Miliroentgen (mR) indicates the most likely level of neutron energy and had a value of 30 meV; the cadmium rate R_{Cd} was 20. This real-time image acquisition system is made of an NE-425 scintillating screen for neutrons. The typical composition is ^{6}LiF + ZnS (~ 0.7 mm thick), which converts the incident neutrons to photons emitted mainly in the green wavelength through the predominant reaction of ^{6}Li(n,α)^{3}H, which emits 1.7×10^5 light photons per neutron detected [7]. We used a Panasonic series WV-CL 920 camera with a 1.27 cm charge coupled device (CCD) (main diagonal) with 580 lines resolution operating with a minimum lighting of 0.02 LUX for lens opening, *f*, of 1.4, which adjusts the integration time of the images. In the optical coupling an $f = 1.0$ MACRO lens manufactured by Canon that allows the manual adjustment of focus was used; in addition to, a plane mirror was placed at a 45° angle to reflect light photons in the direction of the CCD

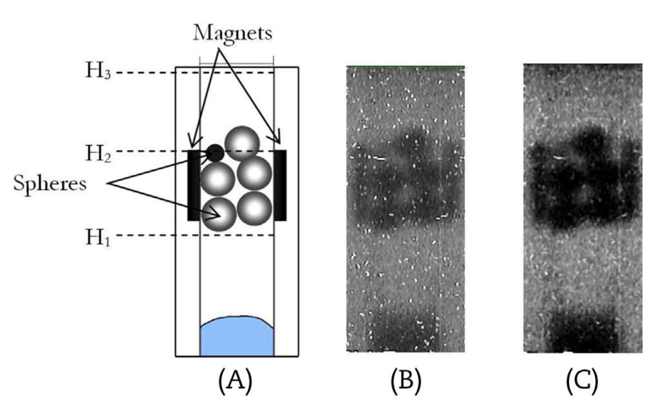

Fig. 2 – Real-time neutron radiography of a metallic pipe with crust. (A) Schematic drawing of the pipe. (B) Image obtained. (C) Previous image after digital processing.

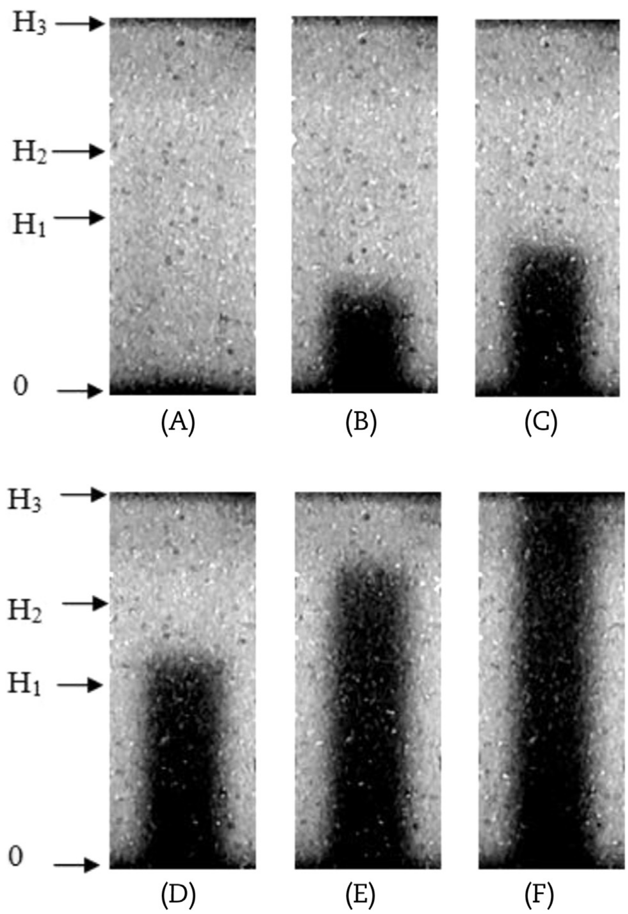

Fig. 3 – Neutron radiographic images in real-time of the aluminum piping. Conditions of (A) empty (without water injection); (B–F) with water in various levels.

camera. The components of the real time EIS were placed in a light-tight box that had an additional shield made of boron paraffin, cadmium, and lead in the area where the CCD camera was positioned. The images were digitalized by a PCTV USB 2.0 external capture plate from Pinnacle with a resolution of 720 × 480 pixels recording 6.0 kbits/s compression in MPEG-2 format through the Vision Version 1.00 software from Pinnacle. The schematic diagram of EIS in real-time and a photograph of EIS system are shown in Fig. 1. The captured neutron radiographic images were converted to AVI format and processed using the Image Pro Plus version 4.0 software.

2.2. *Experimental apparatus*

In order to obtain different images of the crust, an apparatus composed of an injector, an aluminum tube (dimensions of internal diameter: 16.7 mm, thickness: 1.4 mm, and length: 120 cm), a "separating tank" made of transparent acrylic (36.5 cm long and 57.4 cm high), a water leakage meter (R1), an air leakage meter (R2), a hydraulic pump, and an air compressor was designed and built at the exit of the irradiation channel, J-9, of the Argonauta reactor. The water was pumped up by a hydraulic pump whereas the compressor injected air. Five identical steel spheres with diameter of 7.9 mm, coated with a fine cadmium (0.5 mm) cover, and a 6.35 mm sphere without coating were manufactured in order to simulate crust in metallic piping. The spheres were fixed on the internal walls of the aluminum pipe by means of two magnets (~1.4 T each) placed on opposite sides of the pipe in the external wall between heights H_1 and H_2; magnets were placed in such a way as to promote flow resistance, as can be observed in Fig. 2. For these tests, only the water flow meter was turned on, both with spheres and without spheres, and registered a flow speed of 0.9 m/s. Images related to the schematic drawing of the pipe containing the simulated crust, obtained by EIS, as shown in Fig. 2A, are presented in Fig. 2B, which shows the real neutron radiographic image, and in Fig. 2C, which shows the previous image after digital image processing.

Additionally, sequential images of the water flow in the interior of the metallic piping without crust were obtained for comparison to images of the flow in the interior of the pipe after the liquid had passed the simulated crust.

3. Results and discussion

Fig. 3 shows a sequence of real-time neutron radiographic images that indicate the behavior of the flow in the interior of

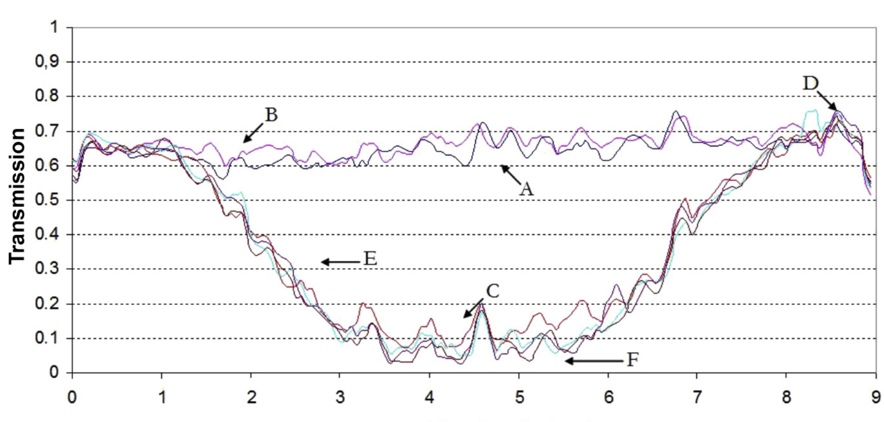

Fig. 4 – Flow profiles along the pipe diameter in the regions below level H_1 (not crust). A–F are lines corresponding to the grayscale of frames registered.

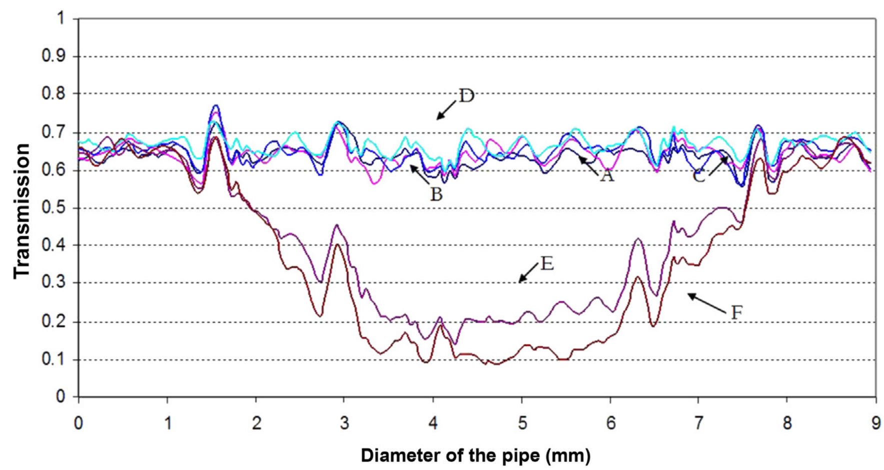

Fig. 5 – Flow profiles along the pipe diameter in regions > level H_2 (not crust). A–F are lines corresponding to the grayscale of frames registered.

the same metallic piping without crust at levels corresponding to heights H_1, H_2, and H_3, respectively, shown in Fig. 3: (A) empty water column at $H = 0$; (B, C) water columns in levels $< H_1$; (D) water column between H_1 and H_2 levels; (E) water columns $> H_2$; and (F) water column at H_3 (full).

For each image sequence shown in Fig. 3, the integrated time allowed was 62.5 ms; this allowed for the building of flow profiles for later comparison with those from pipes with water flow strangled by crust. To build these profiles, two regions were chosen: one at the bottom, below level H_1, and the other just after level H_2. Figs 4 and 5 show the profiles obtained at the analyzed regions, respectively, and show representative curves of the flow behavior along the pipe diameter.

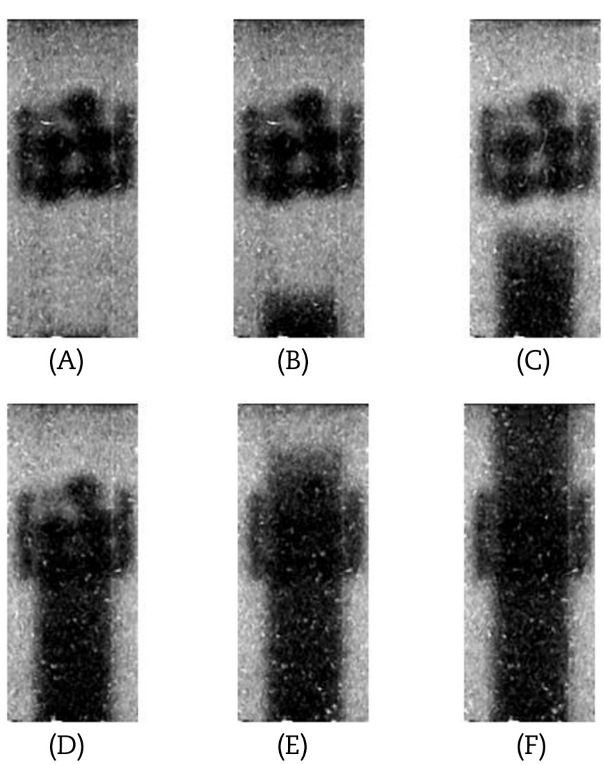

Fig. 6 – Neutron radiographic images in real-time of the crust in the interior of the aluminum pipe. (A) Without water injection. (B–F) Sequences showing the water flowing inside the pipe in the region with the crusts.

Real-time NR images from the water flow in the interior of the metallic piping with crust are shown in the sequence presented in Fig. 6. In a similar way, for the same regions previously selected and with an identical number of frames used in the construction of the profiles shown in Figs. 4 and 5, and curves representing the behavior of the flow along the pipe diameter were obtained from the neutron radiographic images in real-time displayed in Fig. 5.

Figs. 7 and 8 show the profiles obtained in the analyzed regions below and above the crusts, respectively, which refer to the representative curves of the flow behavior along the pipe diameter.

Figs. 4 and 7 show that there is no discrepancy among the flow profiles registered in relation to the crust regions at the inferior part of the tube. However, after the passage of the liquid through these regions, discrepancies between flow profiles increased. The resistance of the crusts to the passage of water is responsible for this behavior. When comparing, for example, the flow profiles represented by lines E and F in Fig. 6, with the corresponding lines (curves E and F) in Fig. 8, this resistance is made evident.

4. Conclusion

Despite the low intensity of the neutron flux, the images obtained showed that the EIS installed at the J-9 channel of the Argonauta/IEN/CNEN reactor [6] is able to perform NR in real-time for the visualization of crust and to obtain flow profiles in metallic piping of small diameter. The tests performed showed that the technique employed is an important tool for nondestructive inspections of parts in industry processes. The images showed the resistance induced by the crusts to the

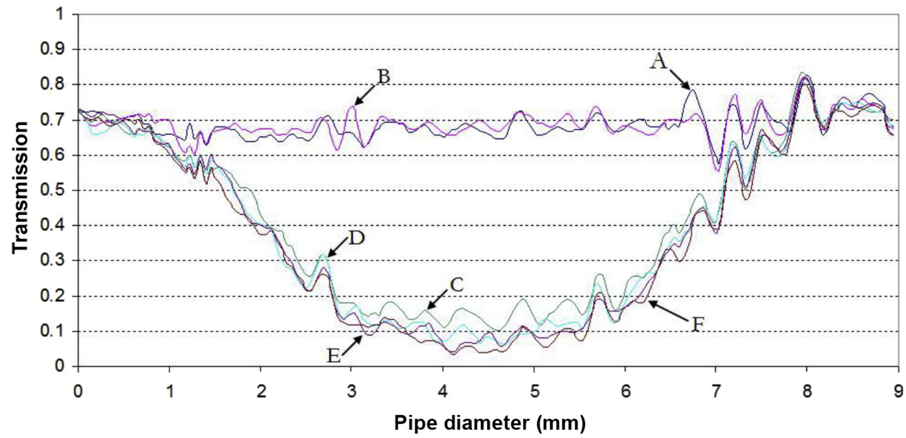

Fig. 7 – Flow profile in the regions below the crust in the pipe. A–F are lines corresponding to the grayscale of frames registered.

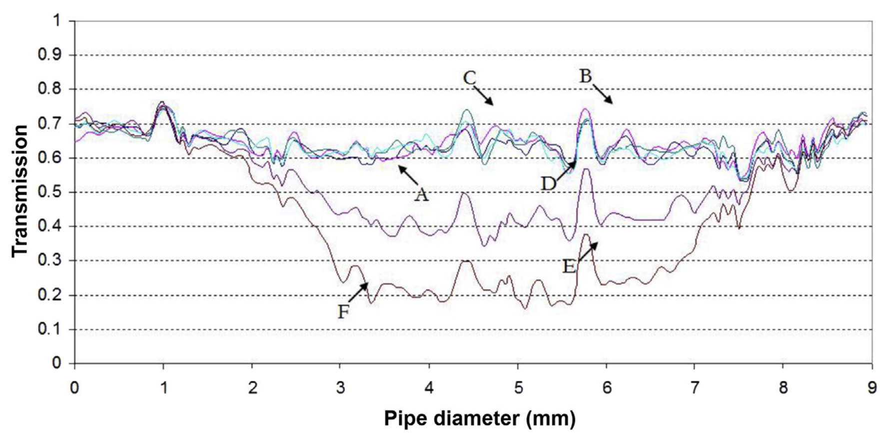

Fig. 8 – Flow profile in the regions above the crust in the pipe. A–F are lines corresponding to the grayscale of frames registered.

passage of water inside the metallic duct through the clear registering of the disturbances that occurred; it was also possible to verify steep discrepancies in the profiles of the representative curves of the flow behavior throughout the pipe diameter. However, in the inferior part of the tube, which has no crust, no disturbance was registered. The tests performed showed that the technique employed is an important tool for nondestructive inspections of parts in the industry process. However, the technique of neutron radiography can be applied in other areas, as has been done by Nuclear Engineer Program at COPPE/UFRJ. An example was the use of the technique to detect drugs and explosives, in Ferreira et al [8].

Conflicts of interest

The authors have no conflicts of interest to declare.

Acknowledgments

We would like to thank the Brazilian funding agency CAPES for financial funding.

REFERENCES

[1] K. Sonada, A. Ono, N. Takenaka, T. Fujii, S. Tazawa, T. Nakani, Visualization and volumetric fraction measurement of multiphase flow by neutron radiography, in: Proceedings of the Fourth World Conference, Gordon and Breach Science Publishers, John P. Barton, San Francisco, California, USA, 1993, pp. 347–354.

[2] W.J. Richards, M.J. Tuttle, K. Ulowetz, R. Mcgee, Real-Time Neutron Radiography – Applications for the Automotive Industry, UCD McClellan Nuclear Radiation Center, UC Davis,

2003. Available from: http://escholarship.org/uc/item/35t9b89n.
[3] H. Berger, Advances in neutron radiographic techniques and applications: a method for nondestructive testing, Appl Radiat Isot 61 (2004) 437–442.
[4] R.C. Lanza, E.W. McFarland, S. Shi, Cooled-CCD and amorphous silicon-based neutron imaging systems for low-fluence neutron sources, in: Proc. SPIE 2867, International Conference Neutrons in Research and Industry 1996, Crete, Greece, 1997, pp. 332–338.
[5] International Atomic Energy Agency (IAEA), IAEA-TECDOC-1604 Neutron Imaging: A Nondestructive Tool for Materials Testing Report of a coordinated research project 2003–2006, IAEA, Vienna, Austria, 2008.
[6] F.J.O. Ferreira, V.R. Crispim, A.X. Silva, Electronic imaging system for neutron radiography at a low power research reactor, Radiat. Meas. 45 (2010) 806–809.
[7] F. Casali, P. Chirco, M. Zanarini, Advanced imaging techniques: the new deal for neutron physics, La Revista del Nuovo Cimento 18 (1995) 1–69.
[8] F.J.O. Ferreira, V.R. Crispim, A.X. Silva, Detection of drugs and explosives using neutron computerized tomography and artificial intelligence technique, Appl Radiat Isot 68 (2010) 1012–1017.

FURTHER READING

[9] M. Ishii, N. Zuber, Drag coefficient and relative velocity in bubbly, droplet, or particulate flows, AlChE 25 (1979) 843–855.
[10] G.B. Wallis, One-Dimensional Two-phase Flow, second ed., McGraw Hill, New York, 1979.
[11] M. Ishii, ONE-dimensional Drift-flux Model and Constitutive Equation for Relative Motion between Phases in Various Two-phase Flow Regimes, Report No. ANL 77-47, Argonne National Lab, Lemont (IL), 1977.
[12] J.G. Collier, Convective Boiling and Condensation, second ed., McGraw Hill, New York, 1981.